

Isoform-specific effects of neuronal repression of the AMPK catalytic subunit on cognitive function in aged mice

Xueyan Zhou^{1,*}, Wenzhong Yang^{1,*}, Xin Wang¹, Tao Ma^{1,2,3}

¹Department of Internal Medicine-Gerontology and Geriatric Medicine, Wake Forest University School of Medicine, Winston-Salem, NC 27157, USA

²Department of Physiology and Pharmacology, Wake Forest University School of Medicine, Winston-Salem, NC 27157, USA

³Department of Neurobiology and Anatomy, Wake Forest University School of Medicine, Winston-Salem, NC 27157, USA

*Equal contribution

Correspondence to: Tao Ma; email: tma@wakehealth.edu

Keywords: AMPK, aging, protein synthesis, learning and memory, proteomics

Received: December 5, 2022

Accepted: February 20, 2023

Published: February 26, 2023

Copyright: © 2023 Zhou et al. This is an open access article distributed under the terms of the [Creative Commons Attribution License](https://creativecommons.org/licenses/by/3.0/) (CC BY 3.0), which permits unrestricted use, distribution, and reproduction in any medium, provided the original author and source are credited.

ABSTRACT

AMP-activated protein kinase (AMPK) functions as a molecular sensor that plays a critical role in maintaining cellular energy homeostasis. Dysregulation of the AMPK signaling has been linked to synaptic failure and cognitive impairments. Our recent study demonstrates abnormally increased AMPK activity in the hippocampus of aged mice. The kinase catalytic subunit of AMPK exists in two isoforms $\alpha 1$ and $\alpha 2$, and their specific roles in aging-related cognitive deficits are unknown. Taking advantage of the unique transgenic mice (AMPK $\alpha 1/\alpha 2$ cKO) recently developed by our group, we investigated how isoform-specific suppression of the neuronal AMPK α may contribute to the regulation of cognitive and synaptic function associated with aging. We found that aging-related impairment of long-term object recognition memory was improved with suppression of AMPK $\alpha 1$ but not AMPK $\alpha 2$ isoform. Moreover, aging-related spatial memory deficits were unaltered with suppression of either AMPK α isoform. Biochemical experiments showed that the phosphorylation levels of the eukaryotic initiation factor 2 α subunit (eIF2 α) were specifically decreased in the hippocampus of the AMPK $\alpha 1$ cKO mice. We further performed large-scale unbiased proteomics analysis and revealed identities of proteins whose expression is differentially regulated with AMPK α isoform suppression. These novel findings may provide insights into the roles of AMPK signaling pathway in cognitive aging.

INTRODUCTION

Normal aging is associated with impairments of multiple aspects of cognitive function [1–4]. Dysregulation of brain energy metabolism has been linked to both the normal aging process and multiple neuronal disorders characterized by cognitive impairments such as Alzheimer's disease (AD) [5–7]. AMP-activated protein kinase (AMPK) functions as a sensor at the molecular levels that plays a crucial role in regulation of cellular energy homeostasis [8]. Mounting evidence suggests a

link between aberrant AMPK signaling and aging-related deficiencies of synaptic plasticity and dementia syndromes [9]. One important downstream effect of AMPK is the regulation of protein synthesis or mRNA translation, which is essential for the long-lasting form of memory and synaptic plasticity [10]. AMPK can regulate mRNA translation through suppression of the mammalian target of rapamycin complex 1 (mTORC1) or phosphorylation and inhibition of the eukaryotic elongation factor 2 (eEF2) by activating its kinase eEF2K [11]. We recently reported that AMPK signaling involves

the phosphorylation of the α subunit of eukaryotic initiation factor 2 (eIF2 α), which may serve as a key underlying molecular mechanism during memory formation [12, 13].

Mammalian AMPK is composed of catalytic α subunit, and β and γ subunits (regulatory). The kinase catalytic subunit has two isoforms $\alpha 1$ and $\alpha 2$ that, are encoded by separate genes (*Prkaa1* and *Prkaa2*) located in distinct chromosomes [14, 15]. AMPK $\alpha 1$ and $\alpha 2$ are both present in the brain, but whether and how regulation of different AMPK α isoforms is involved in neuronal function remain elusive. We recently reported, in young mice (3-6 months old), that neuronal repression of the AMPK $\alpha 2$ (not AMPK $\alpha 1$) results in cognitive defects and long-term synaptic plasticity impairments [12]. Meanwhile, we demonstrated abnormal hyperactive AMPK signaling in the hippocampus of aged mice [2]. In the current study, we aim to investigate how suppression of either AMPK α isoform in neurons may contribute to the regulation of cognitive and synaptic function associated with aging.

MATERIALS AND METHODS

Mice

Mice were housed in a barrier facility at Wake Forest School of Medicine. Operation of the facility complies with standards of the US Department of Agriculture's Animal Welfare Information Center (AWIC), and the NIH Guide for Care and Use of Laboratory Animals. The facility is on a 12-hour light/dark cycle, with a regular cage-cleaning and feeding schedule. Female and male mice were both used. Polymerase chain reaction (PCR) was performed to verify the genotypes.

Mouse behavioral studies

Mice for behavioral studies were handled for 5 days before behavioral testing and habituated for at least 1 hour prior to experiments. Open field (OF) test, Novel object recognition (NOR) test, Morris water maze (MWM) test, visible platform test, and passive avoidance (PA) test were carried out as described [16, 17].

Preparation of acute hippocampal slices and synaptic electrophysiology

Transverse hippocampal slices of 400 μ m thick were prepared as described previously [18]. Slices were maintained at room temperature for at least 2 hours before experimentation in artificial cerebrospinal fluid (ACSF). For synaptic electrophysiology, slices were transferred to preheated (32° C) recording chambers where they were superfused with ACSF. High-frequency

stimulation (HFS, consisting of two 1-sec 100 Hz trains separated by 60 sec) was delivered to induce late-LTP (L-LTP) [12].

Western blots

Brain tissues were dissected, and flash frozen on dry ice. Protocols for Western blot were as described [12]. Resources of antibodies were as described [12].

Surface sensing of translation (SUnSET) assay

Slices were maintained in ACS at room temperature for at least 2 hours before experiments. Slices were further incubated for 1 hour at 32° C in ACSF containing Puromycin (1 μ g/mL). Micro-dissected area CA1 slices were used for Western blot analysis. Puromycin labeled proteins and *de novo* proteins synthesis were detected by using the anti-puromycin antibody, and quantified from the total lane (15 to 250 kDa).

Transmission electron microscopy (TEM)

Protocols for TEM sample preparation and imaging were described in our recent studies [12].

Mass spectrometry (MS)/ proteomic analysis

MS experiments were performed at Rutgers University center for advanced biotechnology and medicine using a Dionex rapid-separation liquid chromatography system interfaced with a QE HF (Thermo Fisher Scientific). Details for MS analysis were described previously [19].

Statistical analysis

Data are presented as mean \pm SEM. A two-tailed unpaired Student's *t*-test was used for two groups comparisons. One-way ANOVA and post hoc tests (when applicable) were used to compare multiple groups. $p < 0.05$ were considered statistically significant. Sample size was based on previous publication [12]. GraphPad Prism software was applied for data analysis. Outliers were assessed by Grubbs test.

RESULTS AND DISCUSSION

Genetic suppression of the neuronal AMPK $\alpha 1$ isoform improves aging-related impairments of recognition memory

We developed the AMPK $\alpha 1/\alpha 2$ cKO mice as described. In these transgenic mice, expression of either the $\alpha 1$ or the $\alpha 2$ isoform is conditionally reduced in excitatory neurons [12]. The mice were aged to 19-22 months old, when multiple aspects of cognition decline in wild-type

(WT) mice [2]. We performed a series of behavioral tasks to assess various cognitive functions in the aged AMPK α 1 cKO and α 2 cKO mice, with the Cre $^{+/-}$ mice as the control. In the open field (OF) test, we did not observe difference among all the three groups of mice in the measurement of periphery duration and travel distance or velocity, indicating unaltered locomotor activities and anxiety levels with suppression of either AMPK α isoforms (Figure 1A–1C). We next performed the novel object recognition (NOR) task to evaluate their long-term recognition memory (24 hours interval between the exploration day and testing day) [20]. In agreement with our previous studies [2], aged Cre $^{+/-}$ mice exhibited impaired recognition memory, as they

did not show a preference for the novel object measured by object interactions (Figure 2A left). Notably, aged AMPK α 1 cKO mice interacted more with novel than with the familiar objects ($p < 0.01$), indicating normal recognition memory (Figure 2A middle). In comparison, aged AMPK α 2 cKO mice displayed a deficiency in recognition memory (Figure 2A right). Interestingly, there is a trend that the aged AMPK α 2 cKO mice spent more time with the familiar object ($p = 0.07$). Results from the analysis of the interactions with the novel objects showed that the long-term recognition memory was improved in the aged AMPK α 1 cKO mice compared to the AMPK α 2 cKO mice ($p < 0.05$) (Figure 2B). There was also a trending

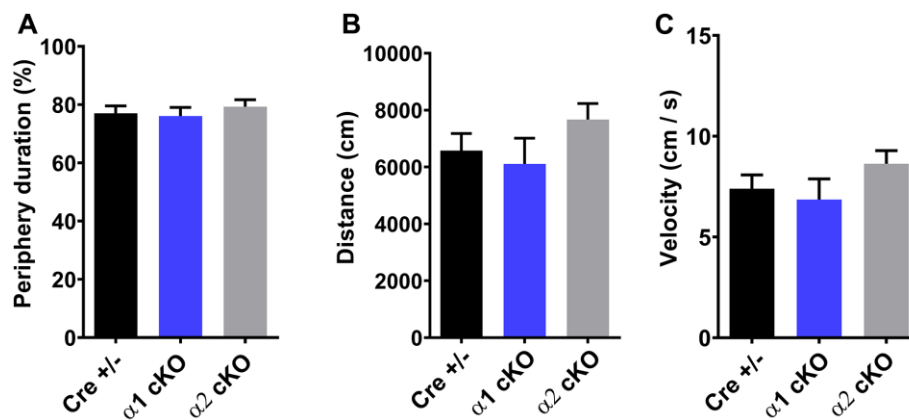


Figure 1. Open field test (OF) showed unaltered periphery duration (A), traveling distance (B), and traveling velocity (C) for both AMPK α 1 cKO and AMPK α 2 cKO mice. $n = 15$ for Cre $^{+/-}$, $n = 13$ for AMPK α 1 cKO, $n = 11$ for AMPK α 2 cKO. $p > 0.05$. One-way ANOVA.

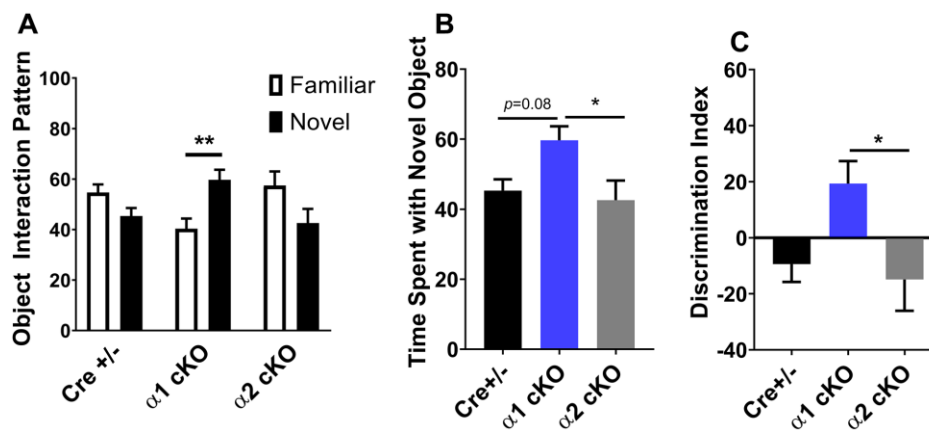


Figure 2. Effects of AMPK α isoform reduction on recognition memory in aged mice. (A) Novel object recognition (NOR) experiments demonstrated that long-term recognition memory was impaired with aging in Cre $^{+/-}$ and AMPK α 2 cKO mice. In contrast, aged AMPK α 1 cKO mice showed normal recognition of novel objects over familiar objects. $n = 8$ for Cre $^{+/-}$ and AMPK α 1 cKO, $n = 10$ for AMPK α 2 cKO. $**p < 0.01$. Unpaired two-tailed t-test. (B) Time spent with the novel object during the NOR test. $n = 8$ for Cre $^{+/-}$ and AMPK α 1 cKO, $n = 10$ for AMPK α 2 cKO. $*p < 0.05$. One-way ANOVA and Tukey's test. (C) NOR discrimination index [(time spent exploring novel object – time spent exploring familiar object) / total exploration time]. $n = 8$ for Cre $^{+/-}$ and AMPK α 1 cKO, $n = 10$ for AMPK α 2 cKO. $*p < 0.05$. One-way ANOVA and Tukey's test.

improvement of recognition memory in the aged AMPK α 1 cKO mice compared to the control mice ($p=0.08$) (Figure 2B). We further analyzed the discrimination index (calculated as time spent with novel object – familiar object) /total interaction time) based on the NOR performance, and confirmed that the aged AMPK α 1 cKO mice exhibited improved recognition memory (positive high index), compared to aging-related impaired cognition in the other two groups (Figure 2C).

Next, we examined the spatial learning/ memory of the mice with the classic Morris water maze (MWM) assay. Consistent with our recent report [2], aged Cre $^{+/-}$ mice exhibited defects in spatial learning and memory indicated by insignificant day-to-day decrease of escapes latency during the learning/training stage (Figure 3A). During the probe trial test, the aged Cre $^{+/-}$ mice also showed reduced target quadrant occupancy and “platform” crossing (Figure 3C and Supplementary Figure 1D). Unlike the results from the

NOR test, both the AMPK α 1 cKO and α 2 cKO mice displayed similar spatial learning/memory impairments during the MWM test compared to the performance of the control group (Figure 3A, 3C and Supplementary Figure 1A, 1D). Further analysis revealed that the performance of the AMPK α 1 cKO mice on day 3 of the MWM training phase was better than that of the AMPK α 2 cKO mice (Figure 3B). In addition, we did not observe differences in swimming distance or velocity during the probe trial test among the three groups of mice (Supplementary Figure 1B, 1C). To evaluate the effects of AMPK α isoform suppression on other non-cognitive factors (e.g. vision, motivation, and swimming ability), we performed a visible platform task in which the escape platform is labeled with a flag and moved between trials [12]. We found that the escape latency during the visible platform test was unaltered in day 2 among all groups (Figure 3D). Interestingly, the Cre $^{+/-}$ mice exhibited shorter escape latency compared to the AMPK α 2 cKO mice in day 1 ($p<0.05$) (Figure 3D).

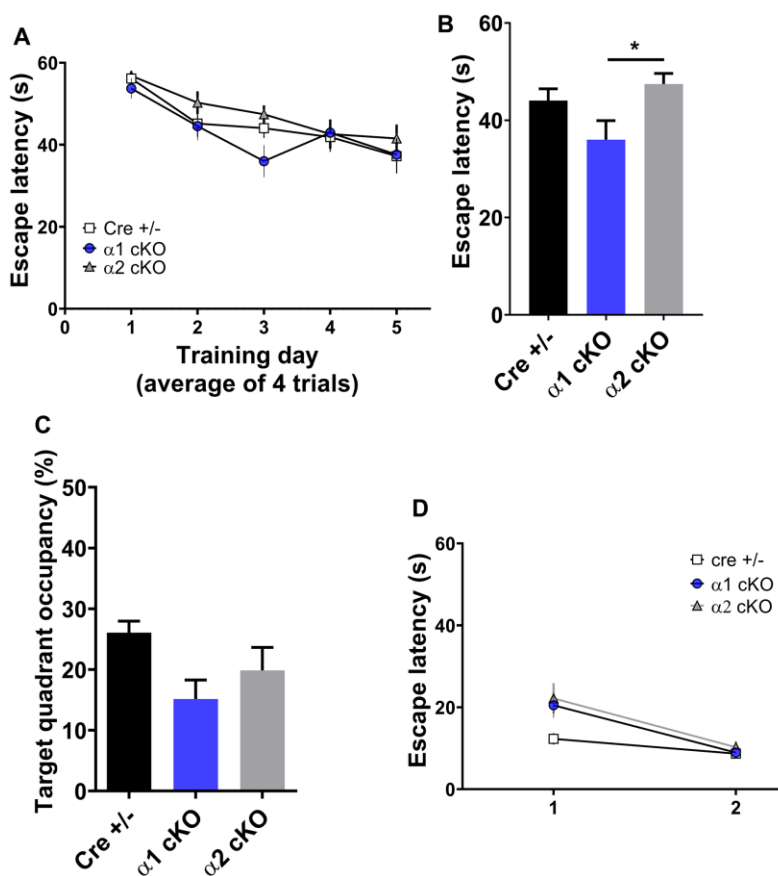


Figure 3. Effects of AMPK α isoform reduction on spatial learning and memory in aged mice. (A) The training phase of the hidden platform Morris water maze (MWM) test showed day-to-day escape latency of the mice. $n=14$ for Cre $^{+/-}$, $n=15$ for AMPK α 1 cKO and AMPK α 2 cKO. $p=0.78$ (interaction between groups). Two-way ANOVA. (B) Escape latency on day 3 of the MWM test. $*p<0.05$. One-way ANOVA and Tukey's test. (C) Measurement of the target quadrant occupancy in the probe trial phase of the MWM test, $n=14$ for Cre $^{+/-}$, $n=15$ for AMPK α 1 cKO and AMPK α 2 cKO. $p=0.056$, One-way ANOVA. (D) Visible platform test. $n=11-15$ mice per group. $p>0.05$ One-way ANOVA.

Additionally, we investigated the effects of AMPK α isoform suppression on the performance of fear-associated learning and memory using the passive avoidance (PA) behavioral task. In the PA task, the mice learn to avoid an environment (measured by the entry latency on the testing day), where they had been shocked a day before (training day). The performance of all three groups of mice was similar during the training day. For the testing day, however, the aged AMPK α 1 cKO mice showed a trend of improved fear learning/memory compared to the aged Cre $^{+/-}$ group ($p=0.06$). Moreover, there is no difference between the AMPK α 2 cKO mice and the control group (Supplementary Figure 2). Combined with the results from the NOR and MWM tests, inhibition of the neuronal AMPK α 1 isoform (but not the AMPK α 2 isoform) can alleviate aging-related impairments of object recognition meanwhile does not improve spatial learning and memory deficits in aged mice. It is known that both the NOR and MWM tests are hippocampal-dependent. However, other brain regions such as prefrontal cortex might play distinct roles in these behavioral tasks [21, 22]. It would be intriguing for future studies to elucidate potential brain-region- or cell type-roles of AMPK α isoforms in aging-related regulation of cognitive function.

Genetic suppression of the neuronal AMPK α 1 isoform does not alter hippocampal long-term synaptic plasticity in aged mice

Furthermore, we examined whether suppression of the AMPK α isoforms affects hippocampal long-term potentiation (LTP), a form of synaptic plasticity that is considered as a cellular model for learning and memory [23]. In this study, we induced protein synthesis-

dependent late LTP by applying a strong electric stimulation protocol [2]. The LTP in the aged Cre $^{+/-}$ mice appeared to be normal (Figure 4), which is consistent with our previous findings in aged wild mice [2]. In addition, the AMPK α 1 cKO and α 2 cKO mice showed similar hippocampal LTP compared to the Cre $^{+/-}$ mice (Figure 4).

Phosphorylation levels of hippocampal eIF2 α in aged mice are reduced by suppression of the neuronal AMPK α 1 isoform in aged mice

We seek to understand molecular mechanisms underlying the behavioral phenotypes associated with the suppression of AMPK α isoforms in aged mice. It has been reported that inhibition of overall AMPK activity results in phosphorylation of eEF2 and/or activation of the mTORC1 signaling, which would increase general protein synthesis [11]. Interestingly, we did not observe alterations of eEF2 phosphorylation in the hippocampus of either the AMPK α 1 cKO or α 2 cKO mice compared to the control group (Figure 5A). In addition, suppression of either AMPK α isoform did not affect the mTORC1 signaling in the hippocampus of the aged mice, as assessed by phosphorylation levels of mTOR (at both Ser2448 and Ser2481 sites), and of the two downstream substrates: p70S6K and 4EBP (Figure 5A and Supplementary Figure 3). Consistently, we also did not observe any significant effects of AMPK α isoform suppression on the phosphorylation levels of AKT, a well-established upstream regulator of mTORC1 (Figure 5A).

We recently reported, in young mice, that reduction of AMPK α 2 results in increased phosphorylation of the eIF2 α , which is associated with inhibition of translational

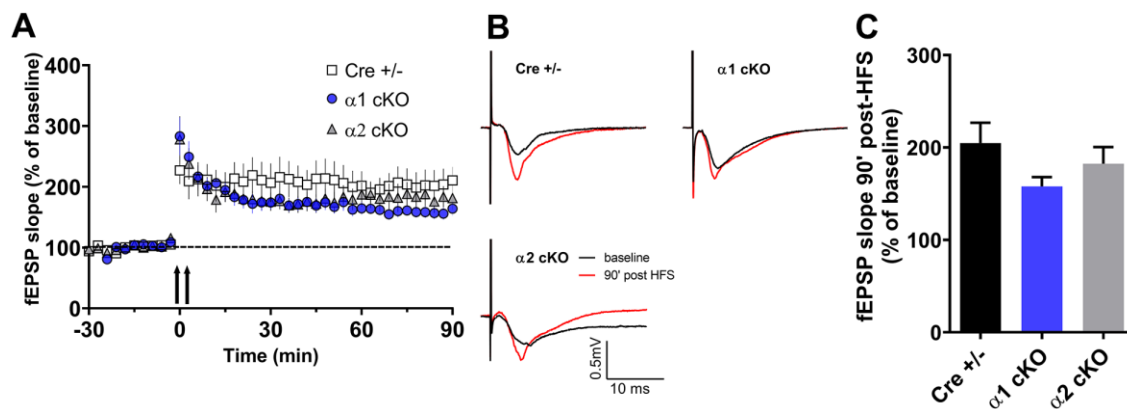


Figure 4. Effects of AMPK α isoform reduction on hippocampal long-term synaptic plasticity in aged mice. (A) Hippocampal late LTP (L-LTP) induced by two-train high-frequency stimulation (HFS, denoted by the arrows). (B) Representative fEPSP traces before and 90 minutes after HFS. (C) Cumulative data showing quantification of mean fEPSP slopes 90 min after delivery of HFS. $n=13$ for Cre $^{+/-}$ and AMPK α 2 cKO, $n=10$ for AMPK α 1 cKO. $p=0.23$, One-way ANOVA.

capacity [12]. In contrast, here we did not observe alterations of eIF2 α phosphorylation in the hippocampus of the aged AMPK α 2 cKO mice compared to the Cre $^{+/-}$ mice group (Figure 5B). Notably, phosphorylation levels of eIF2 α in the hippocampus of the aged AMPK α 1 cKO mice were significantly decreased compared to those in either the control or the AMPK α 2 cKO mice (Figure 5B). We further investigated ATF4, whose expression might be associated with eIF2 α phosphorylation [24, 25]. We did not observe any changes in the protein levels of hippocampal ATF4 in AMPK α 1 or α 2 cKO mice (Figure 5C). Additionally, protein levels of eIF2 α kinase PERK were also unaltered among all the groups (Figure 5D).

Phosphorylation of eIF2 α is considered to result in repression of general protein synthesis [26]. We thus examined de novo protein synthesis in living hippocampal slices by the SUnSET assay [16]. Surprisingly, the results indicate no change of general protein synthesis levels (assessed by puromycin incorporation) among all three groups (Figure 5E). We further carried out transmission electron microscopy experiments to investigate regulation of hippocampal dendritic polyribosomes, an indicator of new protein synthesis [27]. We found that the presence of polyribosomes was unaffected by the suppression of either AMPK α 1 or α 2, compared to the control group (Figure 5F). Potential mechanisms for the unaltered

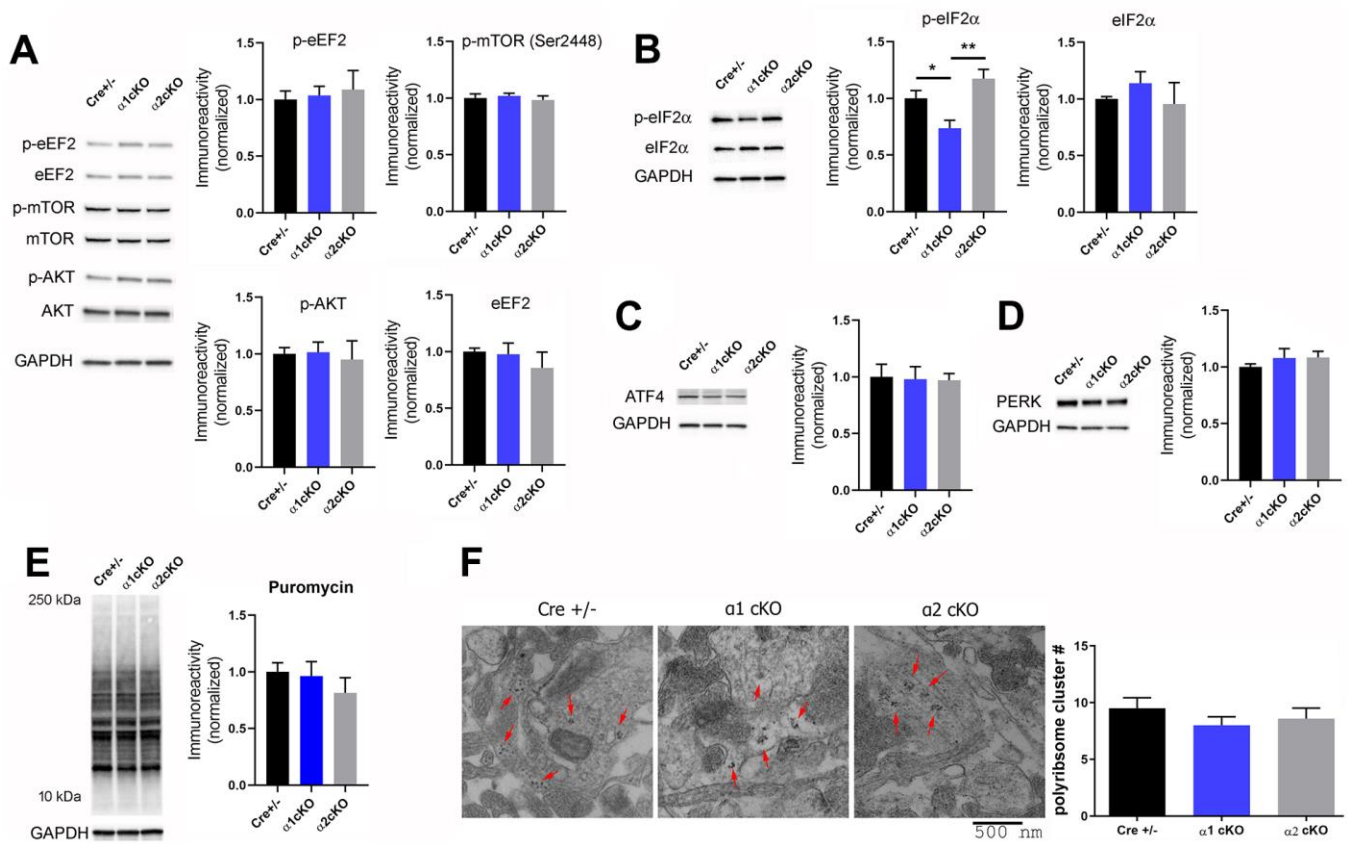


Figure 5. Investigation of signaling pathways associated with AMPK α isoform inhibition in aged mice revealed de-phosphorylation of eIF2 α in the hippocampus of the AMPK α 1 cKO mice. (A) Western blot experiments showed no alterations in phosphorylation levels of eEF2 (Thr56), mTOR (Ser2448), and AKT (Ser473) in hippocampal synaptosome lysate of AMPK α 1 cKO or AMPK α 2 cKO mice, compared to the Cre $^{+/-}$ mice. Representative Western blot gels and quantification data presented in bar graphs are shown. $n = 4-6$ per group. $p > 0.05$, One-way ANOVA. (B) Levels of phospho-eIF2 α (Ser51) were decreased in hippocampal synaptosome lysate of AMPK α 1 cKO mice, compared to Cre $^{+/-}$ or AMPK α 2 cKO mice group. $n = 7-8$ per group. $*p < 0.05$, $**p < 0.01$, One-way ANOVA and Tukey's test. (C, D) Levels of ATF4 and PERK were not altered in either AMPK α 1 cKO or AMPK α 2 cKO mice. $n = 5-6$ per group. $p > 0.05$, One-way ANOVA. (E) Representative images and quantification from the SUnSET de novo protein synthesis assay. $n = 3-4$. $p > 0.05$, One-way ANOVA. (F) Hippocampal polyribosome formation was unaltered in AMPK α 1 cKO or AMPK α 2 cKO mice, compared to the Cre $^{+/-}$ group. Representative transmission electron microscopy (TEM) images of hippocampal CA1 and cumulative data of polyribosome quantification were shown. Polyribosomes were indicated with red arrows. $n = 3$ mice per group (8-10 ROI measurements per mouse). $p = 0.43$. One-way ANOVA.

overall de novo protein synthesis (in consideration of the eIF2 α phosphorylation regulation) may involve the regulation of the protein degradation process and a balance between both upregulation and downregulation of individual protein synthesis (see the proteomics results below). Taken together, suppression of the AMPK α isoform in neurons does not alter the general mRNA translation rate in the hippocampus of aged mice.

Proteomic analysis reveals distinct alterations of protein expression levels associated with suppression of the neuronal AMPK α isoform in aged mice

To gain insights into the potential regulation of the expression of individual proteins associated with the AMPK α isoform reduction, we performed

mass spectrometry (MS)-based proteomic experiments. (Figure 6C, 6D). Most significantly changed hippocampal proteins (up-regulated or down-regulated) in the AMPK α 1 cKO or α 2 cKO mice compared to the Cre $^{+/-}$ mice were shown in Tables 1–4 (illustrated in Supplementary Figure 4). To understand the differences in proteomics between AMPK α 1 cKO and AMPK α 2 cKO mice, we further generated a “volcano” plot to show the fold changes of protein expression levels in the AMPK α 2 cKO mice compared to those in the AMPK α 1 cKO mice (Figure 6B). In brief, levels of 29 proteins were increased and 16 proteins were decreased in the AMPK α 2 cKO mice compared to the AMPK α 1 cKO mice. Detailed lists of these proteins were shown in Tables 5, 6. To further understand how these regulated proteins are involved in different biological processes, we carried out the Gene Ontology (GO)

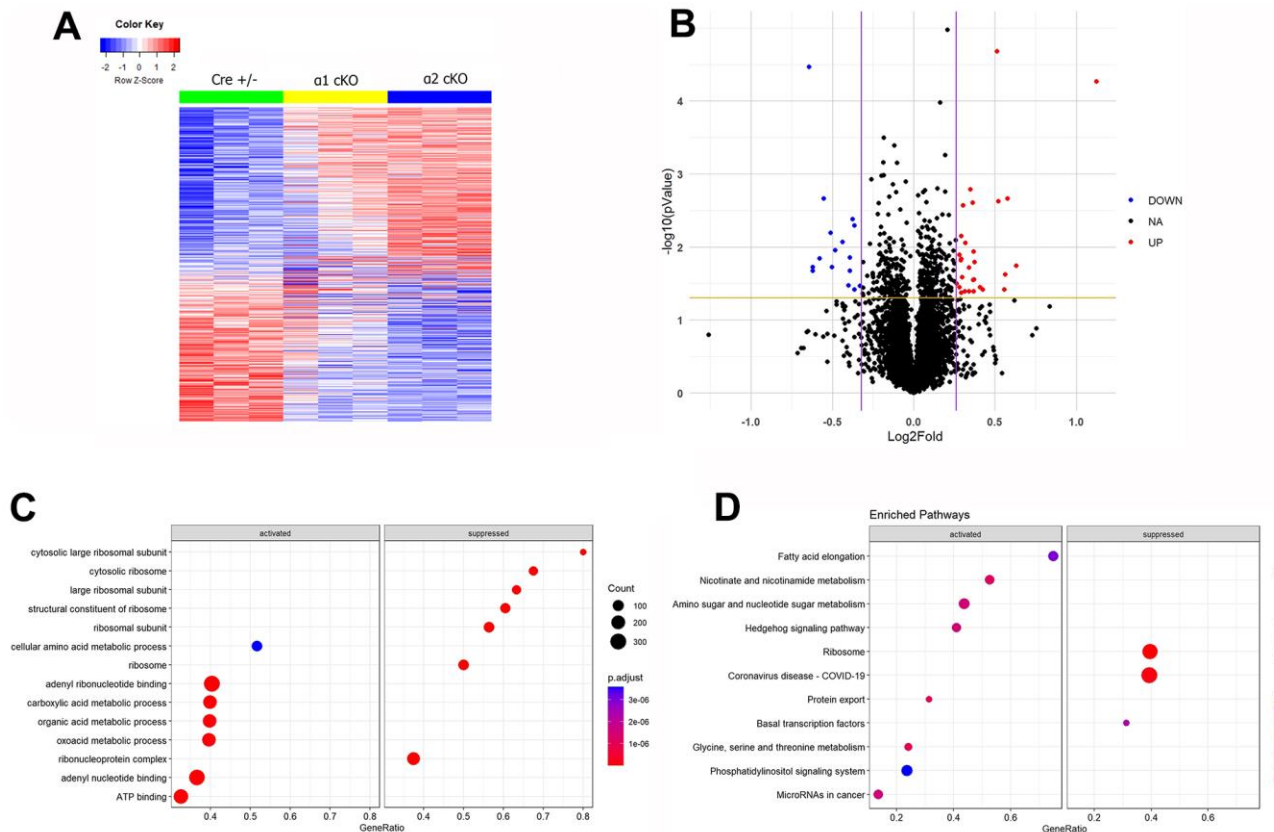


Figure 6. Mass spectrometry (MS)-based proteomics analysis reveals distinct alterations of protein expression levels associated with suppression of the neuronal AMPK α isoform in aged mice. (A) A heat map generated from the MS proteomics data showed the differentially newly synthesized proteins (667 proteins) across the three experimental groups. (B) A volcano plot showed the fold changes of protein expression in AMPK α 2 cKO vs AMPK α 1 cKO mice. Red dots represent those significantly upregulated proteins (29 proteins). Blue dots represent those significantly downregulated proteins (16 proteins). Black dots represent the proteins whose expression levels were not significantly different between the AMPK α 1 cKO and AMPK α 2 cKO mice. (C) Gene Ontology (GO) analysis of the differentially regulated proteins in AMPK α 2 cKO vs AMPK α 1 cKO mice. (D) Gene Set Enrichment Analysis (GSEA) of differentially regulated proteins in AMPK α 2 cKO vs AMPK α 1 cKO mice. All proteomics analysis was performed with the R program. Heat map and volcano plot were generated with ggplot2 package (version 3.3.5) in R (version 4.1.2). GO analysis and GSEA were done with clusterProfiler package (version 4.2.2) in R (version 4.1.2).

Table 1. Top 10 down-regulated proteins in AMPK α 1 cKO mice (compared to Cre+/-).

Protein names	Gene names	P value	Log2Fold
LIM domain and actin-binding protein 1	Lima1	0.013357	-1.02045
Interleukin-34	Il34	0.017373	-0.52683
Peptidyl-prolyl cis-trans isomerase E	Ppie	0.011286	-0.5126
Gamma-aminobutyric acid receptor subunit alpha-4	Gabra4	0.0333	-0.48554
Guanine nucleotide binding protein, beta 2	Gnb2	0.009171	-0.46737
Trafficking protein, kinesin binding 2	Trak2	0.00616	-0.42482
Beta-hexosaminidase subunit alpha	Hexa	0.016773	-0.42092
Cathepsin L1	Ctsl	0.014357	-0.36424
Prospero homeobox protein 1	Prox1	0.003035	-0.33767
Transmembrane emp24 domain-containing protein 5	Tmed5	0.025036	-0.33653

Table 2. Top 10 up-regulated proteins in AMPK α 1 cKO mice (compared to Cre+/-).

Protein names	Gene names	P value	Log2Fold
5-AMP-activated protein kinase subunit beta-1	Prkab1	0.019052	0.423145
GTP-binding protein Rhes	Rasd2	0.034253	0.437368
Tropomyosin alpha-1 chain	Tpm1	0.021857	0.448768
Dynein light chain 2, cytoplasmic	Dynll2	0.045608	0.468517
Palmitoyltransferase	Zdhhc8	0.015551	0.523234
Ubiquitin-conjugating enzyme E2 D1	Ube2d1	0.0454	0.578678
Short transient receptor potential channel 6	Trpc6	0.006422	0.607953
Progressive ankylosis protein	Ank	0.00454	0.803404
FAD-dependent oxidoreductase domain-containing protein 2	Foxred2	0.002152	0.919643
Nuclear factor NF-kappa-B p100 subunit	Nfkb2	0.00424	2.891302

Table 3. Top 10 down-regulated proteins in in AMPK α 2 cKO mice (compared to Cre+/-).

Protein names	Gene names	P value	Log2Fold
NAD(P) transhydrogenase, mitochondrial	Nnt	0.00093	-1.12257
LIM domain and actin-binding protein 1	Lima1	0.011128	-1.05596
U1 small nuclear ribonucleoprotein C	Snrpc	0.030598	-0.88195
Centrosomal protein of 290 kDa	Cep290	0.03503	-0.85265
Peroxiredoxin 5	Prdx5	0.004656	-0.7859
Serine protease inhibitor A3B	Serpina3b	0.001913	-0.76149
Tubulin alpha chain-like 3	Tubal3	0.012086	-0.73929
U6 snRNA-associated Sm-like protein LSM7	Lsm7	0.031444	-0.72817
Transmembrane emp24 domain-containing protein 5	Tmed5	0.002663	-0.69864
N6-adenosine-methyltransferase subunit METTL14	Mettl14	0.046065	-0.65453

Table 4. Top 10 up-regulated proteins in in AMPK α 2 cKO mice (compared to Cre+/-).

Protein names	Gene names	P value	Log2Fold
Coiled-coil domain-containing protein 97	Ccdc97	0.000594	0.833568
Transmembrane protein 69	Tmem69	0.022074	0.959761
Putative hydroxypyruvate isomerase	Hyi	0.000394	0.971629
Histone deacetylase 3	Hdac3	0.002509	0.982715
Myosin-10	Myh10	0.003434	0.996647

Putative tyrosine-protein phosphatase auxilin	Dnaja6	0.014514	1.097624
Progressive ankylosis protein	Ank	0.000313	1.211377
Internexin neuronal intermediate filament protein, alpha	Ina	0.006883	1.231642
Dedicator of cytokinesis protein 6	Dock6	0.006143	1.297596
Nuclear factor NF-kappa-B p100 subunit	Nfkb2	0.000778	3.381316

Table 5. Up-regulated proteins in AMPK α 2 cKO mice compared to AMPK α 1 cKO mice.

Protein names	Gene names	P value	Log2Fold
Putative hydroxypyruvate isomerase	Hyi	<0.0001	1.13
propionyl-CoA carboxylase subunit beta	Pccb	0.0182	0.63
Ribonuclease P protein subunit p14	Rpp14	0.0022	0.58
Histone deacetylase 3	Hdac3	0.0239	0.56
Dedicator of cytokinesis protein 6	Dock6	0.0384	0.56
Haloacid dehalogenase-like hydrolase domain-containing protein 3	Hdhd3	0.0024	0.52
Insulin-degrading enzyme	Ide	<0.0001	0.51
Methyl-CpG-binding domain protein 2	Mbd2	0.0382	0.43
Adiponectin receptor protein	Adipor	0.0356	0.41
Delta-aminolevulinic acid dehydratase	Alad	0.0163	0.38
Complement C4 beta chain	C4b	0.0280	0.37
Activity-regulated cytoskeleton-associated protein	Arc	0.0116	0.37
ETS domain-containing transcription factor	Erf	0.0406	0.37
Vasculin	Gbp1	0.0283	0.37
Probable proline--tRNA ligase, mitochondrial	Pars2	0.0025	0.36
Glycogen synthase, muscle	Gys1	0.0016	0.35
1,2-dihydroxy-3-keto-5-methylthiopentene dioxygenase	Adi1	0.0192	0.34
Dual specificity testis-specific protein kinase 1	Tesk1	0.0405	0.34
Transmembrane protein 168	Tmem168	0.0088	0.32
trafficking protein, kinesin binding 2	Trak2	0.0410	0.31
Hydroxypyruvate isomerase	Hyi	0.0027	0.30
Glutamate-rich WD repeat-containing protein 1	Grwd1	0.0263	0.30
T-box brain protein 1	Tbr1	0.0424	0.29
Oligoribonuclease, mitochondrial	Rexo2	0.0071	0.29
Probable ATP-dependent RNA helicase DDX58	Ddx58	0.0147	0.29
Uncharacterized protein CXorf38 homolog	1810030O07Rik	0.0153	0.29
Sodium bicarbonate cotransporter 3	Slc4a7	0.0360	0.28
Cyclin-L2	Ccnl2	0.0129	0.28
Cytosolic endo-beta-N-acetylglucosaminidase	Engase	0.0318	0.27

Table 6. Down-regulated proteins in AMPK α 2 cKO mice compared to AMPK α 1 cKO mice.

Protein names	Gene names	P value	Log2Fold
5-AMP-activated protein kinase catalytic subunit alpha-2	Prkaa2	<0.0001	-0.64
Calmodulin-binding transcription activator 2	Camta2	0.0214	-0.62
WD repeat and FYVE domain containing 1	Wdfy1	0.0191	-0.62
Aminoacylase-1	Acy1	0.0145	-0.58
Protein FAM177A1	Fam177a1	0.0021	-0.55

Disks large-associated protein 1	Dlgap1	0.0064	-0.51
Necdin	Ndn	0.0189	-0.50
UDP-N-acetylglucosamine transferase subunit ALG14 homolog	Alg14	0.0111	-0.48
FYVE, RhoGEF and PH domain-containing protein 5	Fgd5	0.0086	-0.44
RNA binding protein fox-1 homolog 1	Rbfox1	0.0340	-0.40
Codanin-1	Cdan1	0.0213	-0.39
Bone morphogenetic protein receptor type-1B	Bmpr1b	0.0139	-0.39
3-ketoacyl-CoA thiolase A, peroxisomal	Acaa1a	0.0042	-0.38
Vesicle-associated membrane protein 4	Vamp4	0.0384	-0.36
Transmembrane emp24 domain-containing protein 5	Tmed5	0.0051	-0.36
Ig heavy chain V	Ighv	0.0342	-0.33

analysis and the Gene Set Enrichment Analysis (GSEA) in AMPK α 2 cKO and AMPK α 1 cKO mice (Figure 6C, 6D). GO analysis of the differentially regulated proteins between AMPK α 1 cKO and AMPK α 2 cKO mice suggested that expression of proteins involved in the biological processes related to ribosome subunit biology was suppressed in the AMPK α 2 cKO mice compared to AMPK α 1 cKO mice. In contrast, expression of proteins involved in the metabolism-related processes was activated in the AMPK α 2 cKO mice compared to AMPK α 1 cKO mice (Figure 6C). Consistent with GO analysis, GSEA analysis shows that ribosome-related pathways were suppressed, while metabolism-related pathways were activated in AMPK α 2 cKO mice compared to AMPK α 1 cKO mice (Figure 6D). Interestingly, we found COVID-19-related pathways were suppressed in the AMPK α 2 cKO mice, suggesting AMPK α isoforms may play distinct role in viral infection (Figure 6D).

CONCLUSIONS

In summary, the current study reported that suppression of neuronal AMPK α 1 isoform can improve aging-related impairments of long-term recognition memory. Together with our previous studies in characterizing the young AMPK α transgenic mice, these novel findings point to a previously unrecognized role of AMPK α isoform homeostasis in cognition during development. The study indicates that the aging process might have distinct impact on the signaling pathways associated with the AMPK α isoforms, and future studies are necessary to determine the underlying mechanisms. Finally, it is appealing for future studies to explore whether targeting AMPK α isoform regulation could be a feasible strategy to mitigate aging-related cognitive impairments.

AUTHOR CONTRIBUTIONS

XZ, WY, XW and TM conceived and designed the study. XZ, WY, and XW performed the experiments.

TM wrote the first draft of the manuscript. All authors contributed to the final draft of the manuscript.

ACKNOWLEDGMENTS

We thank Dr. Haiyan Zheng at the center for advanced biotechnology and medicine of Rutgers University for her tremendous help on proteomics analysis. We thank the Wake Forest School of Medicine Pathology and Imaging Core for their help with tissue processing and technical help with imaging experiments.

CONFLICTS OF INTEREST

The authors declare that they have no conflicts of interest.

ETHICAL STATEMENT

All animal procedures were conducted in accordance with the standards and policies set by the US Department of Agriculture's Animal Welfare Information Center (AWIC), and the NIH Guide for Care and Use of Laboratory Animals, with the approval of Wake Forest University School of Medicine Institutional Animal Care and Use Committee (IACUC).

FUNDING

This work was supported by National Institutes of Health grants R01 AG055581, R01 AG056622, and R01 AG073823 (T.M.).

REFERENCES

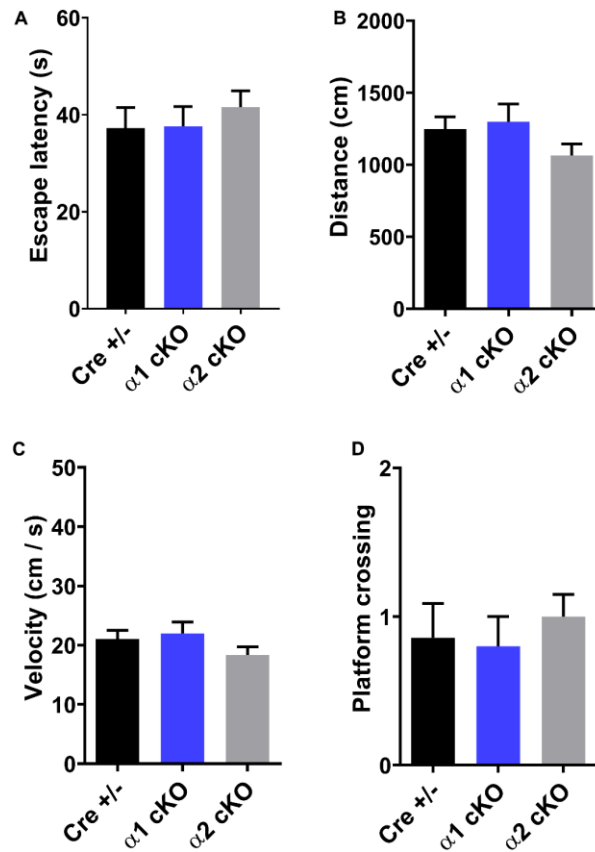
- Burke SN, Barnes CA. Neural plasticity in the ageing brain. *Nat Rev Neurosci.* 2006; 7:30–40. <https://doi.org/10.1038/nrn1809> PMID:16371948
- Yang W, Zhou X, Ma T. Memory Decline and Behavioral Inflexibility in Aged Mice Are Correlated With

- Dysregulation of Protein Synthesis Capacity. *Front Aging Neurosci.* 2019; 11:246.
<https://doi.org/10.3389/fnagi.2019.00246>
PMID:31551760
3. Klencklen G, Després O, Dufour A. What do we know about aging and spatial cognition? Reviews and perspectives. *Ageing Res Rev.* 2012; 11:123–35.
<https://doi.org/10.1016/j.arr.2011.10.001>
PMID:22085884
 4. Hedden T, Gabrieli JD. Insights into the ageing mind: a view from cognitive neuroscience. *Nat Rev Neurosci.* 2004; 5:87–96.
<https://doi.org/10.1038/nrn1323> PMID:14735112
 5. Lin MT, Beal MF. Mitochondrial dysfunction and oxidative stress in neurodegenerative diseases. *Nature.* 2006; 443:787–95.
<https://doi.org/10.1038/nature05292> PMID:17051205
 6. Błaszczyk JW. Energy Metabolism Decline in the Aging Brain-Pathogenesis of Neurodegenerative Disorders. *Metabolites.* 2020; 10:450.
<https://doi.org/10.3390/metabo10110450>
PMID:33171879
 7. Ryu JC, Zimmer ER, Rosa-Neto P, Yoon SO. Consequences of Metabolic Disruption in Alzheimer's Disease Pathology. *Neurotherapeutics.* 2019; 16:600–10.
<https://doi.org/10.1007/s13311-019-00755-y>
PMID:31270743
 8. Hardie DG, Ross FA, Hawley SA. AMPK: a nutrient and energy sensor that maintains energy homeostasis. *Nat Rev Mol Cell Biol.* 2012; 13:251–62.
<https://doi.org/10.1038/nrm3311> PMID:22436748
 9. Wang X, Zimmermann HR, Ma T. Therapeutic Potential of AMP-Activated Protein Kinase in Alzheimer's Disease. *J Alzheimers Dis.* 2019; 68:33–8.
<https://doi.org/10.3233/JAD-181043> PMID:30776001
 10. Sossin WS, Costa-Mattioli M. Translational Control in the Brain in Health and Disease. *Cold Spring Harb Perspect Biol.* 2019; 11:a032912.
<https://doi.org/10.1101/cshperspect.a032912>
PMID:30082469
 11. Steinberg GR, Kemp BE. AMPK in Health and Disease. *Physiol Rev.* 2009; 89:1025–78.
<https://doi.org/10.1152/physrev.00011.2008>
PMID:19584320
 12. Yang W, Zhou X, Zimmermann HR, Ma T. Brain-specific suppression of AMPK α 2 isoform impairs cognition and hippocampal LTP by PERK-mediated eIF2 α phosphorylation. *Mol Psychiatry.* 2021; 26:1880–97.
<https://doi.org/10.1038/s41380-020-0739-z>
PMID:32366952
 13. Costa-Mattioli M, Gobert D, Stern E, Gamache K, Colina R, Cuello C, Sossin W, Kaufman R, Pelletier J, Rosenblum K, Krnjević K, Lacaille JC, Nader K, Sonenberg N. eIF2 α phosphorylation bidirectionally regulates the switch from short- to long-term synaptic plasticity and memory. *Cell.* 2007; 129:195–206.
<https://doi.org/10.1016/j.cell.2007.01.050>
PMID:17418795
 14. Hardie DG. AMPK--sensing energy while talking to other signaling pathways. *Cell Metab.* 2014; 20:939–52.
<https://doi.org/10.1016/j.cmet.2014.09.013>
PMID:25448702
 15. Viollet B, Horman S, Leclerc J, Lantier L, Foretz M, Billaud M, Giri S, Andreelli F. AMPK inhibition in health and disease. *Crit Rev Biochem Mol Biol.* 2010; 45:276–95.
<https://doi.org/10.3109/10409238.2010.488215>
PMID:20522000
 16. Gosrani SP, Jester HM, Zhou X, Ryazanov AG, Ma T. Repression of eEF2 kinase improves deficits in novel object recognition memory in aged mice. *Neurobiol Aging.* 2020; 95:154–60.
<https://doi.org/10.1016/j.neurobiolaging.2020.07.016>
PMID:32810756
 17. Day SM, Yang W, Wang X, Stern JE, Zhou X, Macauley SL, Ma T. Glucagon-Like Peptide-1 Cleavage Product Improves Cognitive Function in a Mouse Model of Down Syndrome. *eNeuro.* 2019; 6.
<https://doi.org/10.1523/ENEURO.0031-19.2019>
PMID:31040160
 18. Yang W, Zhou X, Ryazanov AG, Ma T. Suppression of the kinase for elongation factor 2 alleviates mGluR-LTD impairments in a mouse model of Alzheimer's disease. *Neurobiol Aging.* 2021; 98:225–30.
<https://doi.org/10.1016/j.neurobiolaging.2020.11.016>
PMID:33341653
 19. Sleat DE, Sun P, Wiseman JA, Huang L, El-Banna M, Zheng H, Moore DF, Lobel P. Extending the mannose 6-phosphate glycoproteome by high resolution/accuracy mass spectrometry analysis of control and acid phosphatase 5-deficient mice. *Mol Cell Proteomics.* 2013; 12:1806–17.
<https://doi.org/10.1074/mcp.M112.026179>
PMID:23478313
 20. Beckelman BC, Yang W, Kasica NP, Zimmermann HR, Zhou X, Keene CD, Ryazanov AG, Ma T. Genetic reduction of eEF2 kinase alleviates pathophysiology in Alzheimer's disease model mice. *J Clin Invest.* 2019; 129:820–33.
<https://doi.org/10.1172/JCI122954>
PMID:30667373

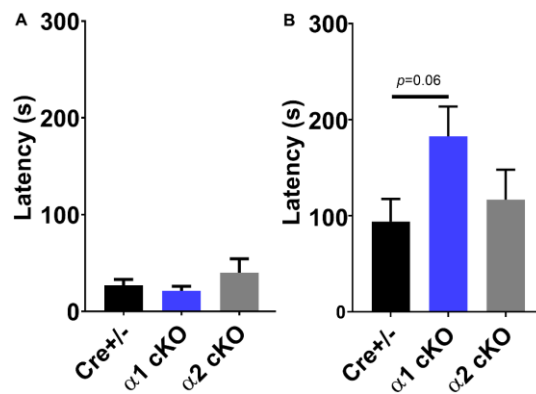
21. Akirav I, Maroun M. Ventromedial prefrontal cortex is obligatory for consolidation and reconsolidation of object recognition memory. *Cereb Cortex*. 2006; 16:1759–65.
<https://doi.org/10.1093/cercor/bhj114>
PMID:[16421330](https://pubmed.ncbi.nlm.nih.gov/16421330/)
22. Buzsáki G, Moser EI. Memory, navigation and theta rhythm in the hippocampal-entorhinal system. *Nat Neurosci*. 2013; 16:130–8.
<https://doi.org/10.1038/nn.3304>
PMID:[23354386](https://pubmed.ncbi.nlm.nih.gov/23354386/)
23. Bliss TV, Collingridge GL. A synaptic model of memory: long-term potentiation in the hippocampus. *Nature*. 1993; 361:31–9.
<https://doi.org/10.1038/361031a0>
PMID:[8421494](https://pubmed.ncbi.nlm.nih.gov/8421494/)
24. Trinh MA, Kaphzan H, Wek RC, Pierre P, Cavener DR, Klann E. Brain-specific disruption of the eIF2 α kinase PERK decreases ATF4 expression and impairs behavioral flexibility. *Cell Rep*. 2012; 1:676–88.
<https://doi.org/10.1016/j.celrep.2012.04.010>
PMID:[22813743](https://pubmed.ncbi.nlm.nih.gov/22813743/)
25. Wek RC, Cavener DR. Translational control and the unfolded protein response. *Antioxid Redox Signal*. 2007; 9:2357–71.
<https://doi.org/10.1089/ars.2007.1764>
PMID:[17760508](https://pubmed.ncbi.nlm.nih.gov/17760508/)
26. Wek RC. Role of eIF2 α Kinases in Translational Control and Adaptation to Cellular Stress. *Cold Spring Harb Perspect Biol*. 2018; 10:a032870.
<https://doi.org/10.1101/cshperspect.a032870>
PMID:[29440070](https://pubmed.ncbi.nlm.nih.gov/29440070/)
27. Ostroff LE, Botsford B, Gindina S, Cowansage KK, LeDoux JE, Klann E, Hoeffler C. Accumulation of Polyribosomes in Dendritic Spine Heads, But Not Bases and Necks, during Memory Consolidation Depends on Cap-Dependent Translation Initiation. *J Neurosci*. 2017; 37:1862–72.
<https://doi.org/10.1523/JNEUROSCI.3301-16.2017>
PMID:[28087764](https://pubmed.ncbi.nlm.nih.gov/28087764/)

SUPPLEMENTARY MATERIALS

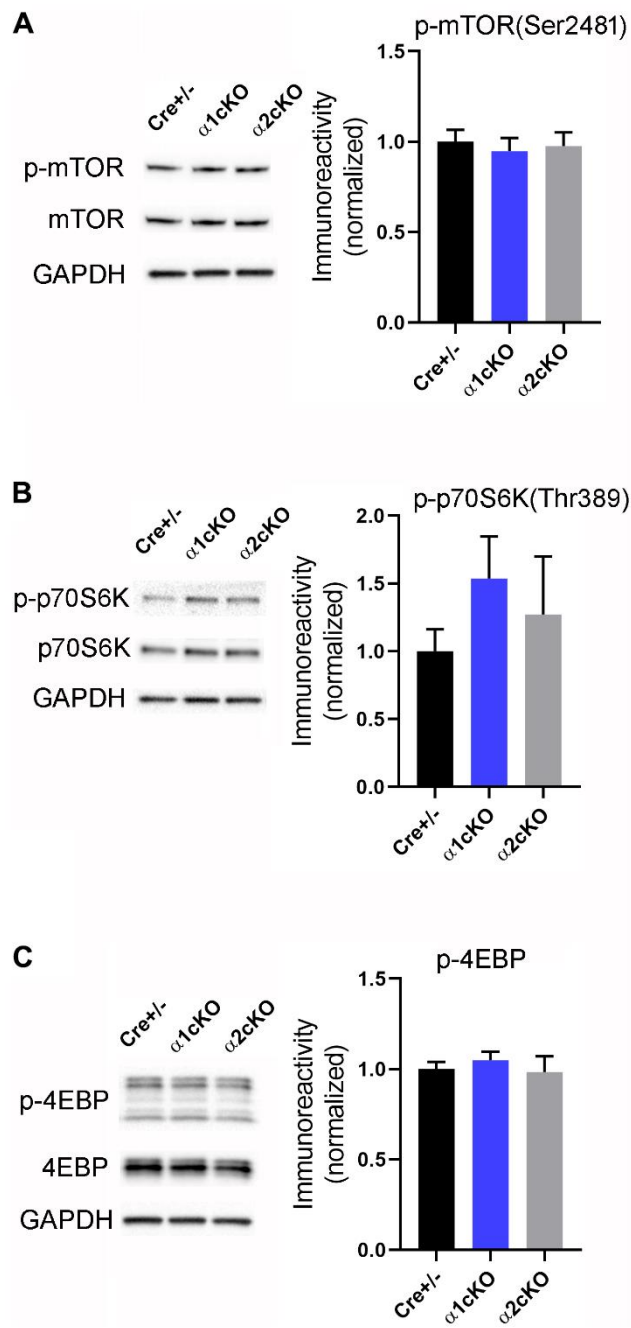
Supplementary Figures



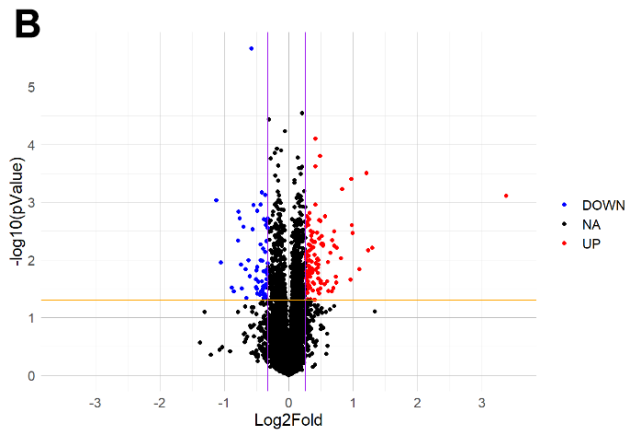
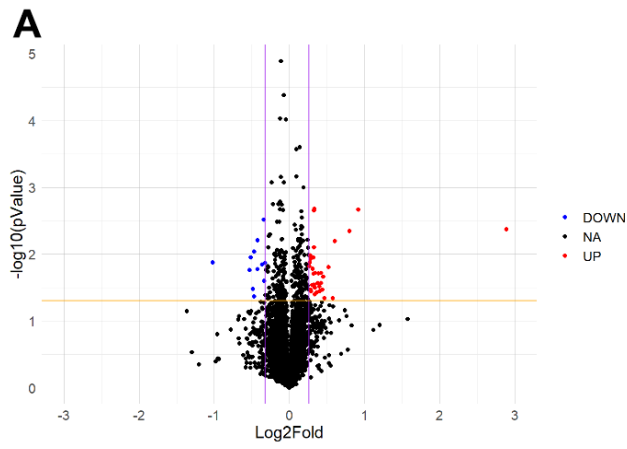
Supplementary Figure 1. Characterization of behavioral phenotypes in aged transgenic mice with AMPKα isoform suppression. (A) Escape latency on day 5 of the MWM test. (B) Swimming distance during the probe trial of the MWM test. (C) Swimming velocity during the MWM probe trial. (D) Measurement of “platform” crossing in the probe trial of the MWM test. , n=14 for Cre+/-, n=15 for AMPKα1 cKO and AMPKα2 cKO. $p=0.22$, One-way ANOVA.



Supplementary Figure 2. Effects of AMPKα isoform reduction on fear-associated memory in aged mice. (A) Training day of the passive avoidance (PA) test. (B) Testing Day of the PA task. n=18 for Cre+/- and AMPKα1 cKO, n=13 for AMPKα2 cKO. One-way ANOVA and Tukey’s test.



Supplementary Figure 3. Examination of the mTORC1 signaling pathway in the hippocampus of the transgenic mice with AMPK α isoform suppression. Western blot experiments showed no alterations in phosphorylation levels of (A) mTOR (Ser2481), (B) p70S6K (Thr389), and (C) 4EBP. Representative Western blot gels and quantification data presented in bar graphs are shown. n=5-6 per group. $p > 0.05$ One-way ANOVA.



Supplementary Figure 4. Volcano plot showed the fold changes of protein expression in AMPK α 1 cKO vs. Cre $^{+/-}$ (A) and AMPK α 2 cKO vs. Cre $^{+/-}$ mice (B). Red dots represent those significantly upregulated proteins. Blue dots represent those significantly downregulated proteins. Black dots represent the proteins whose expression levels were not significantly altered.